A PORTABLE MAGNETO-OPTICAL TRAP

by

Raymond T. Newell

A thesis submitted in partial fulfillment
of the requirements for the degree of

Master of Science
in Physics

at the

UNIVERSITY OF WISCONSIN- MADISON

1998

Abstract

We have created a portable magneto-optical trapping system. This device is capable of cooling approximately 10^6 Rubidium atoms to temperatures in the hundreds of microkelvins. The entire ensemble weighs approximately 50 pounds and requires roughly one hour to set up. It is therefore well-suited to travelling demonstrations and advanced undergraduate teaching labs.

Acknowledgments

This project would not have possible without the support of a great many people, to whom I am sincerely grateful. Naturally my advisor, Thad Walker, tops the list. Thad put me in a challenging research position when I arrived at graduate school and has supplied me with work, encouragement, and resources throughout my time here. Working with Thad has taught me a great deal about atomic physics and its study. Thank you for giving me so many challenges and opportunities.

My friend and colleague, Bien Chann, has made a tremendous contribution to this project for which I am quite grateful. Bien's skills with laser diodes are unparalleled and I thank him for sharing his knowledge with me. More than this, Bien's irreverent good humor and relaxed, confident attitude have made the stresses of this past semester so much more pleasant. I wish him the best in graduate school and in his upcoming marriage.

As near as I can tell, nothing good ever happened without some help from Renée Nesnidal. She has always been happy to put aside her own work to answer a question, find a half-wave plate, eat a donut, or talk through something on my mind. I am tremendously thankful for all the guidance she has given me.

Steve Kadlecek is a uniquely talented physicist. I admire his determination to solve the hard problems and understand the underlying principles. He was always eager to help me troubleshoot a circuit or figure out what Thad was talking about. Sharing a lab with Ian Nelson was a great joy. His strong sense of humor and library of wacky stories made endless hours in the dark pass quickly. I was especially pleased to share the stage with these two talented performers in the Madison Follies. I trust I'll be contacted when plans for the World Tour are finalized.

The time I spent working with Paul Voytas will not soon be forgotten. Paul's knowledge of experimental equipment and techniques is astonishing, though his clear explainations always made it look easy. I envy the students of Wittenberg their Professor Voytas.

The Experimental Nuclear Physics group has given me a great deal of help and encouragement throughout my time here. Paul Quin, Tom Wise and Tom Finnessy have all provided a great deal of logistical and moral support to my endeavors.

Finally, my compañeros John Peck, Brad Frazer, Jason Meaux, Brian Lepore and Bryan Fry have provided the support and friendship that have kept me going throughout this project. The Magnificent Six will ride again.

It has been an honor and a pleasure to be a part of the UW-Madison Atom Trainers

Table of Contents

ABSTRACT ..... **II**

Acknowledgments ..... *iii*

Table of Contents ..... *iv*

Table of Figures ..... *vi*

INTRODUCTION AND BACKGROUND **7**

VISCOUS LIGHT FORCE 7

ZEEMAN-SHIFT SPRING FORCE 10

PYRAMIDAL MIRRORS 11

APPARATUS **13**

LASER SYSTEM 14

Construction *14*

OPTICAL SYSTEM 17

POLARIZATION SPECTROSCOPY 20

Theory *20*

Construction and Analysis *22*

ELECTRONICS 23

Power supplies *25*

Laser Diode Driver *25*

Thermoelectric Cooler Controller *26*

CCD Camera *27*

Microwave Modulation *28*

Ramp Generator and Current to Voltage Converter *29*

Locking Circuit *30*

VACUUM SYSTEM 31

Design *31*

Gas Load Analysis *33*

Construction and Characterization *34*

PYRAMIDAL MIRROR 36

PERMANENT MAGNETS 37

SET-UP AND USE **39**

CONCLUSIONS AND OUTLOOK **41**

BIBLIOGRAPHY **42**

Table of Figures

FIGURE 1 ATOM BETWEEN TWO DETUNED LASER BEAMS..... 8

FIGURE 2 PROBABILITY OF ABSORPTION VS. FREQUENCY 8

FIGURE 3 ENERGY LEVEL DIAGRAM FOR $5^2S_{1/2}$ AND $5^2P_{3/2}$ LEVELS IN ^{85}RB 9

FIGURE 4 ENERGY LEVELS SPLIT BY MAGNETIC FIELD..... 10

FIGURE 5 ORIENTATION OF LASERS AND FIELD COILS FOR A MOT 11

FIGURE 6 RIGHT HOLLOW PYRAMIDAL MIRROR ASSEMBLY (FROM WILLIAMSON, 1997)..... 12

FIGURE 7 OVERVIEW OF APPARATUS..... 13

FIGURE 8 LASER HEAD ASSEMBLY, SEEN FROM ABOVE..... 15

FIGURE 9 SIDE VIEW OF THE LASER HEAD ASSEMBLY 16

FIGURE 10 TOP VIEW OF LASER HOUSING AND BASEPLATE..... 17

FIGURE 11 ORIENTATION OF DIODE CRYSTAL AND LASER OUTPUT 18

FIGURE 12 POLARIZATION SPECTROSCOPY WITH THE ZEEMAN SHIFT [CORWIN *ET AL* 1998}..... 20

FIGURE 13 ORIENTATION OF PHOTODIODES IN POLARIZATION SPECTROSCOPY SET-UP 22

FIGURE 14 POLARIZATION SPECTROSCOPY APPARATUS, SEEN FROM ABOVE..... 22

FIGURE 15 OVERVIEW OF CONTROL ELECTRONICS 24

FIGURE 16 POWER CONNECTIONS AT LASER DIODE..... 26

FIGURE 17 CCD CAMERA POWER SUPPLY..... 27

FIGURE 18 LOCKING CIRCUIT SCHEMATIC 30

FIGURE 19 VACUUM CHAMBER, SEEN FROM ABOVE..... 32

FIGURE 20 CLOSE-UP OF FUNNEL ASSEMBLY IN VACUUM CHAMBER..... 33

FIGURE 21 ION PUMP CALIBRATION SCHEMATIC..... 35

FIGURE 22 ION PUMP CALIBRATION..... 35

FIGURE 23 PERMANENT MAGNET USED TO REPRODUCE AN ANTI-HELMHOLTZ FIELD 37

FIGURE 24 STOKES' CONSTRUCTION FOR FIELD OF PERMANENT MAGNETS 38

FIGURE 25 DIFFERENTIAL ABSORPTION SIGNAL [FROM CORWIN *ET AL*, 1998]..... 40

Introduction and Background

Since the first demonstration of three-dimensional confinement by Steven Chu *et al.* [1986] at AT&T Bell Labs, the science of magneto-optical trapping has advanced rapidly. The ability to isolate, confine and cool large numbers of atoms has been a boon to many areas of physics research, including the study of inter-atomic forces, internal atomic structure and quantum macrostates. The tremendous interest in atom trapping has led to several advances in the necessary technologies and techniques. Basic atom traps have grown simpler and less expensive, so that they are now frequently employed in undergraduate curricula [C. Wieman et al. 1992]. It seemed natural to take advantage of several recent developments in the field by constructing a trapping apparatus that is small enough to be readily transported. As an added benefit, the self-contained laser from this system would be ideally suited to quick and convenient use in other research projects.

As the field has grown, a number of excellent review articles have been published, including those by C.J. Foot [1991], and S. Chu and C. Wieman [1989]. Consequently, this text will not attempt a comprehensive discussion of the physics underlying magneto-optical trapping. Rather, a general background emphasizing those points relevant to this project will be presented. Specifically, the nature of the viscous light force, the central Zeeman force, and the experimental equipment needed to produce them will be discussed.

Viscous Light Force

For simplicity, consider a hypothetical atom with only two energy levels sitting a one-dimensional space. Let us suppose that this space is illuminated with two counter-propagating laser beams at a frequency ν_L which is slightly less than the resonant frequency of the atomic transition ν_0. In the parlance of atom trapping, the frequency difference $\nu_L - \nu_0$ is known as the detuning. If the atom moves with a certain velocity v in the -x direction, it will see a Doppler shift in the frequency of the two laser beams. Specifically, the beam travelling in the -x direction will appear to be at a frequency $\nu_L - \kappa v$, while the beam travelling in the +x direction will have frequency $\nu_L + \kappa v$.

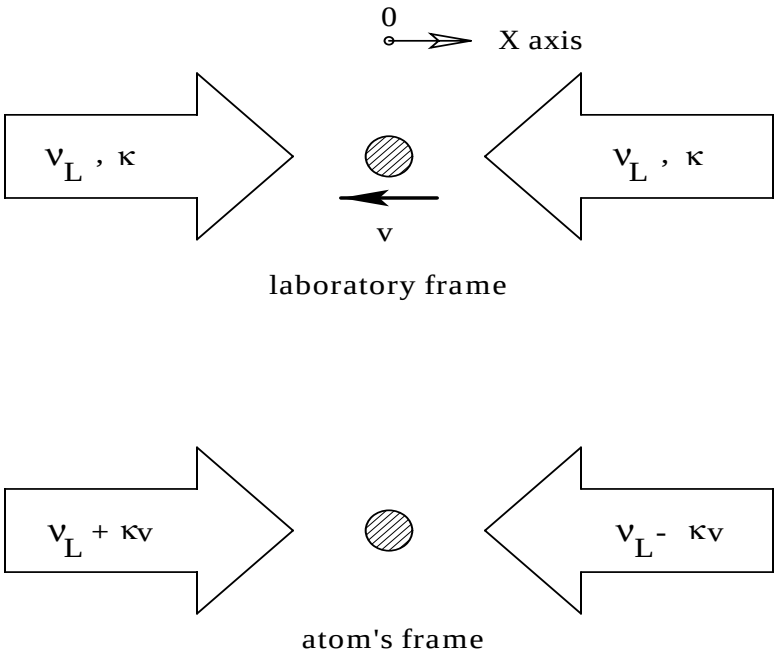

Figure 1 Atom between two detuned laser beams

Since the unshifted laser frequency ν_L was a little below resonance, the +x laser is more nearly resonant with the atom than the -x laser, and the atom will preferentially absorb photons from it.

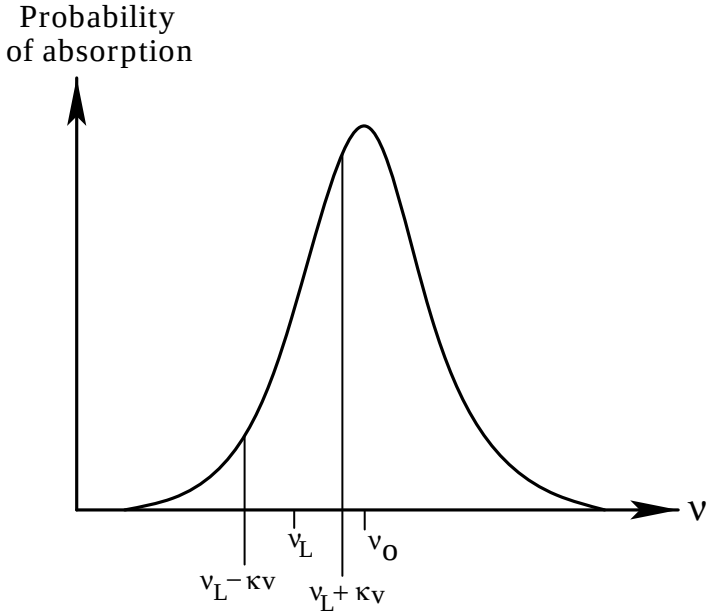

Figure 2 Probability of absorption vs. frequency

As a result of this preferential absorption, the atom receives a net momentum kick that opposes its initial momentum. If the absorption imbalance is large enough, the atom's motion will be significantly retarded. It is not difficult to extrapolate from this one-dimensional case to our three-dimensional world. We need only include four more laser beams, so that we have a pair of counter propagating beams along each of the three Cartesian axes. In this manner one can achieve an "optical molasses" in which atoms automatically feel a radiation pressure opposing their movement.

Unfortunately, real atoms are a bit more complicated than our hypothetical two-level model. Some accommodation must be made for the multitude of energy levels present in any atom. Indeed, trapping becomes extremely difficult as the number of levels increases; this provides strong motivation to trap atoms with simple electronic structures like the alkalis and alkali earths. In this apparatus as in many others, rubidium is chosen because its structure is relatively simple and well understood. We use the $5^2S_{1/2}$ F=3 to $5^2P_{3/2}$ F'=4 transition for trapping, which requires laser light at 780 nm.

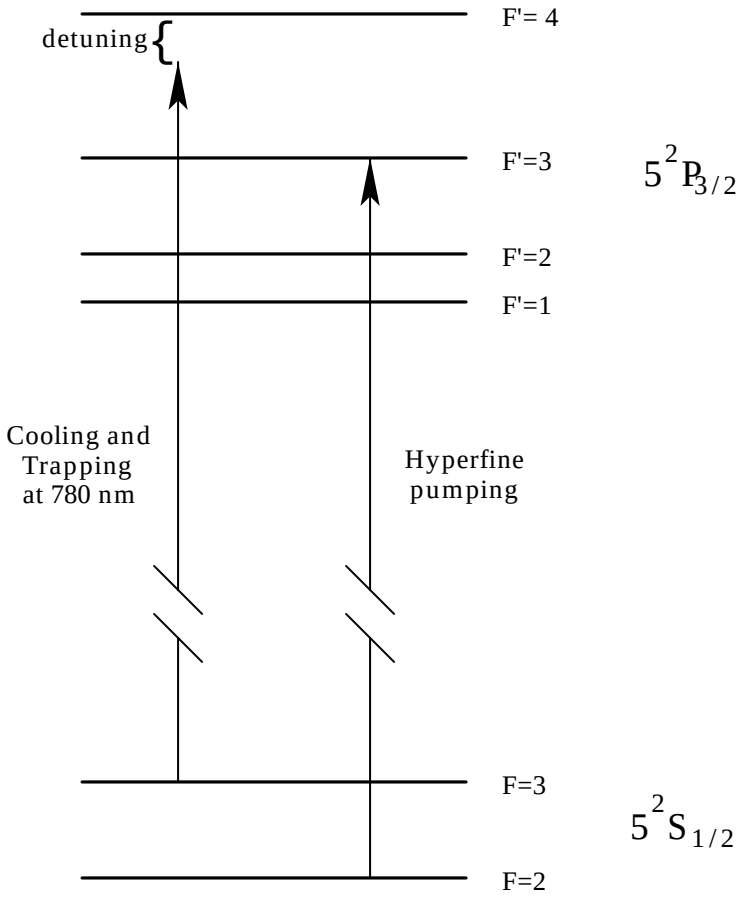

Figure 3 Energy level diagram for $5^2S_{1/2}$ and $5^2P_{3/2}$ levels in ^{85}Rb

Once excited to the F'=4 level, the atom is likely to decay back to the F=3 level, but there is a small chance it will make a transition to the F=2 level. Such a transition poses a problem, because the atom is then no longer nearly resonant with the 780 nm light. Having fallen into this "dark" state, the atom is not likely to absorb any more photons and all cooling halts. Since we require thousands of resonant absorptions to achieve effective trapping, we must do something to pump the atom out of this dark state so that it can continue to absorb 780 nm light. The problem is easily solved by including a small amount of light that is resonant with the $5^2S_{1/2}$ F=2 to $5^2P_{3/2}$ F'=3 transition. With this second "hyperfine pumping" frequency included, we are able to keep the atoms cycling through the trapping transition almost all the time.

Zeeman-Shift spring force

The optical molasses method is good for reducing the average velocity of a collection of atoms, but it is not yet a trap. To trap atoms we must not only cool them but also confine them to a small region of space with some sort of centering force. This can be done fairly simply with the application of a suitable magnetic field and appropriate polarization of the lasers.

To see how it works, return to the two-level atom in a one-dimensional space. Let us apply a linear magnetic field that passes through zero at the origin, and let us suppose that the two laser beams have been given opposite circular polarizations. The magnetic field will split the m_F sublevels in the upper electronic level through the Zeeman interaction: the stronger the field, the larger the splitting.

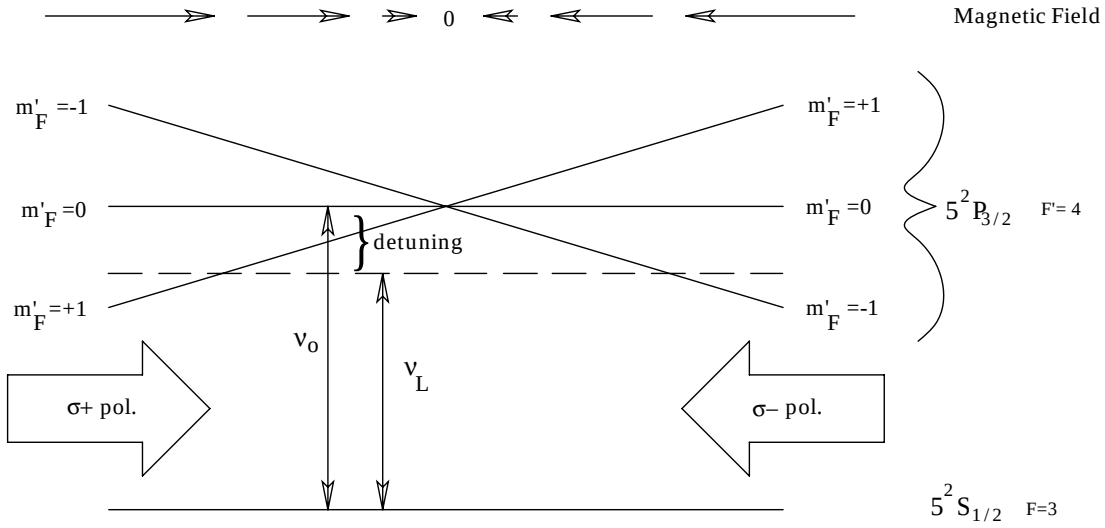

Figure 4 Energy levels split by magnetic field

On the +x side the magnetic field is positive, so the $m'_F = -1$ level is shifted to a lower energy, making it more nearly resonant with the detuned laser light. The $m'_F = +1$ level is shifted up, further from resonance with the laser. Thus, photons which are able to stimulate transitions from $m_F = 0$ to $m'_F = -1$ (σ^- polarized) are more likely to be absorbed than those which stimulate transitions to $m'_F = +1$ (σ^+ polarized). If the laser beam propagating in the -x direction is σ^- polarized and the +x beam is σ^+, atoms on the +x side of the origin will feel a force imbalance pushing them toward the center. On the -x side, the magnetic field is reversed, so the level splitting is reversed, and atoms feel a force in the +x direction. We have thus created the centering force necessary for a trap.

Pyramidal Mirrors

Through the viscous light force and the Zeeman centering force it is possible to cool and trap atoms with a suitable arrangement of detuned laser beams and a magnetic field. Specifically, we need a pair of circularly polarized counter-propagating beams along each of the three Cartesian axes and a quadrupole magnetic field.

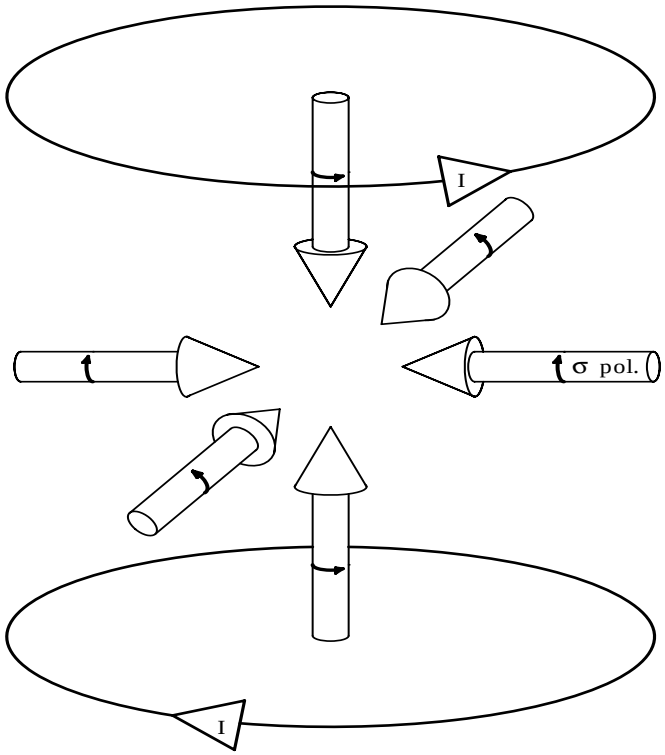

Figure 5 Orientation of lasers and field coils for a MOT

K. I. Lee *et al* [1996] described a method for producing the correct configuration of laser beams by illuminating a hollow pyramidal arrangement of mirrors. Subsequent work by R.S. Williamson, P. Voytas, T. Walker and myself developed the technique to the level implemented here. A single beam of circularly polarized light fills the entire pyramid with light. Rays entering on one side are reflected across the center after striking one mirror and are then reflected back out after striking the other. A counter-propagating set of rays is created by the complementary ray entering on the other side of pyramid. Since 45° reflections off of a gold surface approximately reverse the helicity of the light, the circular polarization works out as well.

In this project we have used this pyramidal mirror arrangement to create a magneto-optical trapping system that is compact enough to be transported and set up outside an optics laboratory environment.

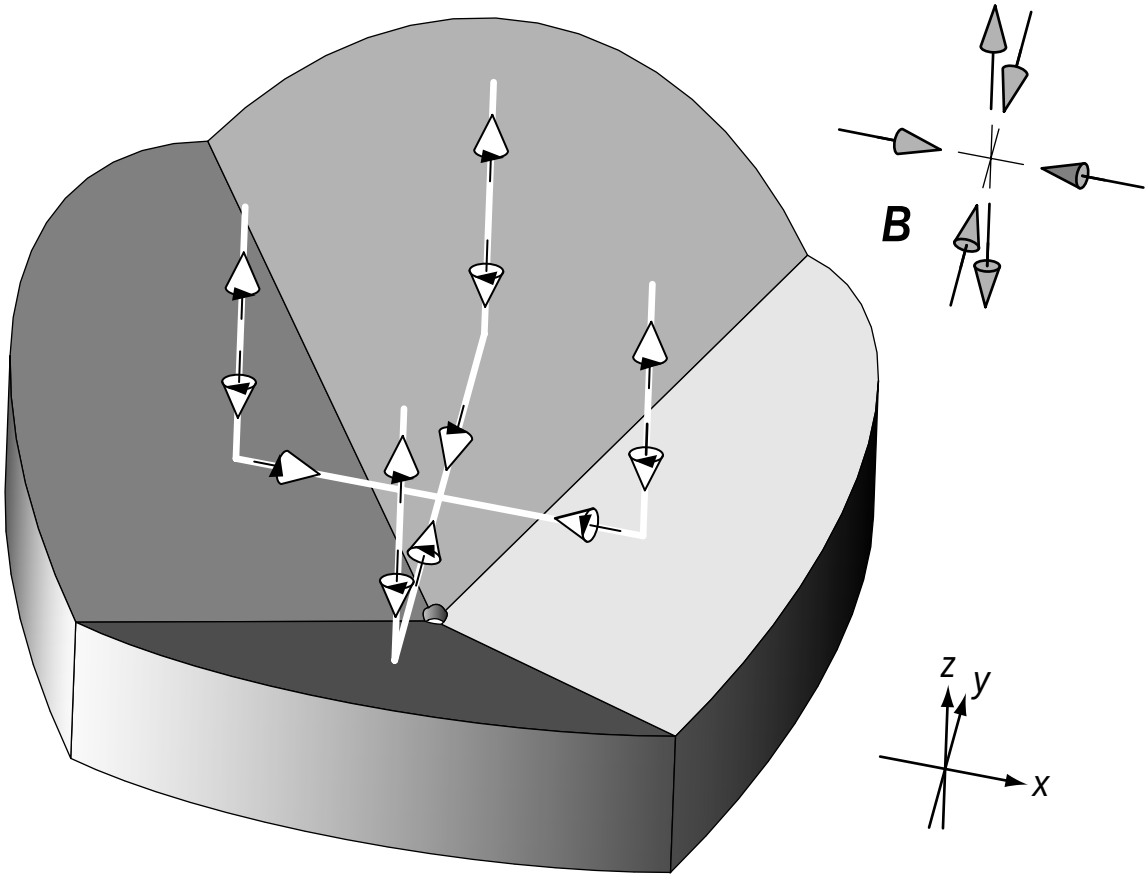

Figure 6 Right hollow pyramidal mirror assembly (from Williamson, 1997)

Apparatus

Our trapping system consists of two main assemblies; an optical rail holding the laser, spectroscopy set-up and beam shaping elements, and a vacuum chamber containing the pyramidal mirrors and permanent magnets. The control and driving electronics are contained a box that plugs into the laser head. With the addition of a standard video monitor with a BNC signal input, the system is ready to create and display a cloud of ultracold rubidium atoms.

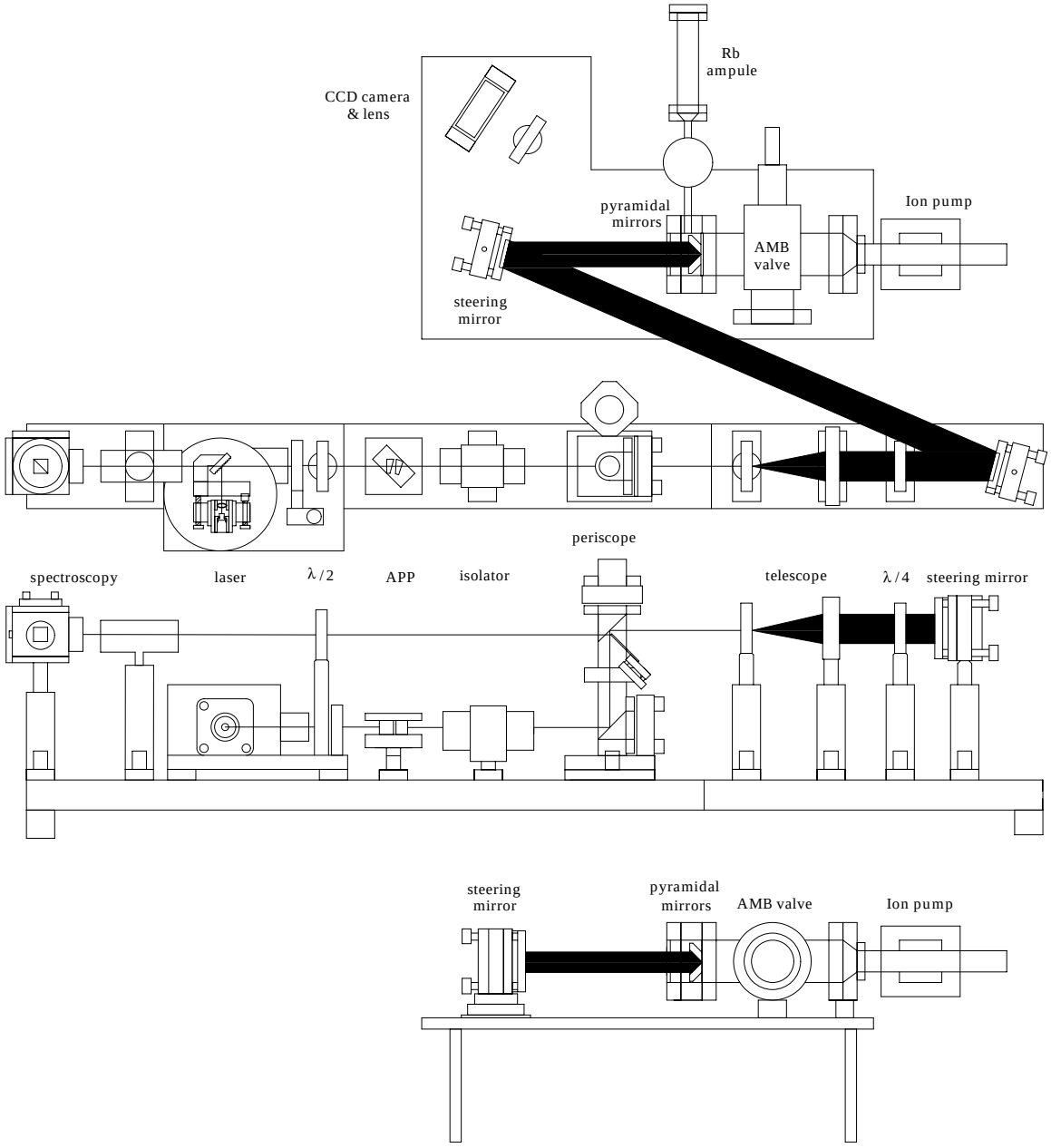

Figure 7 Overview of Apparatus

Laser system

To achieve magneto-optical trapping a laser system must meet several requirements. Primary among these is a highly stable output frequency. Since the operation of the trap requires a constant source of light that is detuned a few MHz from resonance, the laser output must be stable to within one MHz or so. This challenge can be met with commercially available laser diodes placed in a frequency selective resonant cavity. Without feedback, a standard diode will lase in many different modes and produce an unacceptably large linewidth. However, if a small amount of the laser output is fed back into the laser crystal it will cause the crystal to lase at the frequency of the feedback signal. A popular way to take advantage of this property is to place a diffraction grating in the Littrow configuration in front of the diode [Wieman and Hollberg, 1991]. The first-order diffraction pattern will send a small amount of light back into the diode and provide frequency selective optical feedback. Slight changes in the angle of the diffraction grating lead to changes in the frequency of the feedback, and thereby allow tuning of the laser output.

Construction

We have constructed a laser system that works in this manner. The design closely follows the work of A. S. Arnold et al. at the Sussex Centre of Optical and Atomic Physics [A.S. Arnold *et al*., 1998]. A Sharp LT 025 MD laser diode and a collimating lens are placed in a collimation tube (Thorlabs LT 110P-B). The diode is held firmly in place by a retaining ring and the lens can be moved in and out by rotating it in the tube. It is not difficult to move the lens to a position such that the laser beam is well-collimated and retains its profile over large distances.

The collimating tube is fixed to the back plate of a Newport U100-P mirror mount. This is achieved with minor modification of the UPA-PA1 adapter that comes with the mirror mount. Modification of the front plate allows attachment of a grating holder that locates the grating in the laser beam. This arrangement permits fine adjustment of the grating angle by means of the mirror mount's HPS-80 steering screws. A piezo-electric translator (Thorlabs AE0505D08) placed between one of the steering screws and the front plate allows electronic control of the grating angle. It is best to rotate the collimating tube in its holder so that the wide axis of the laser beam is horizontal. The beam then sees a larger

number of diffraction gratings and the angular resolution of the first diffracted order is higher.

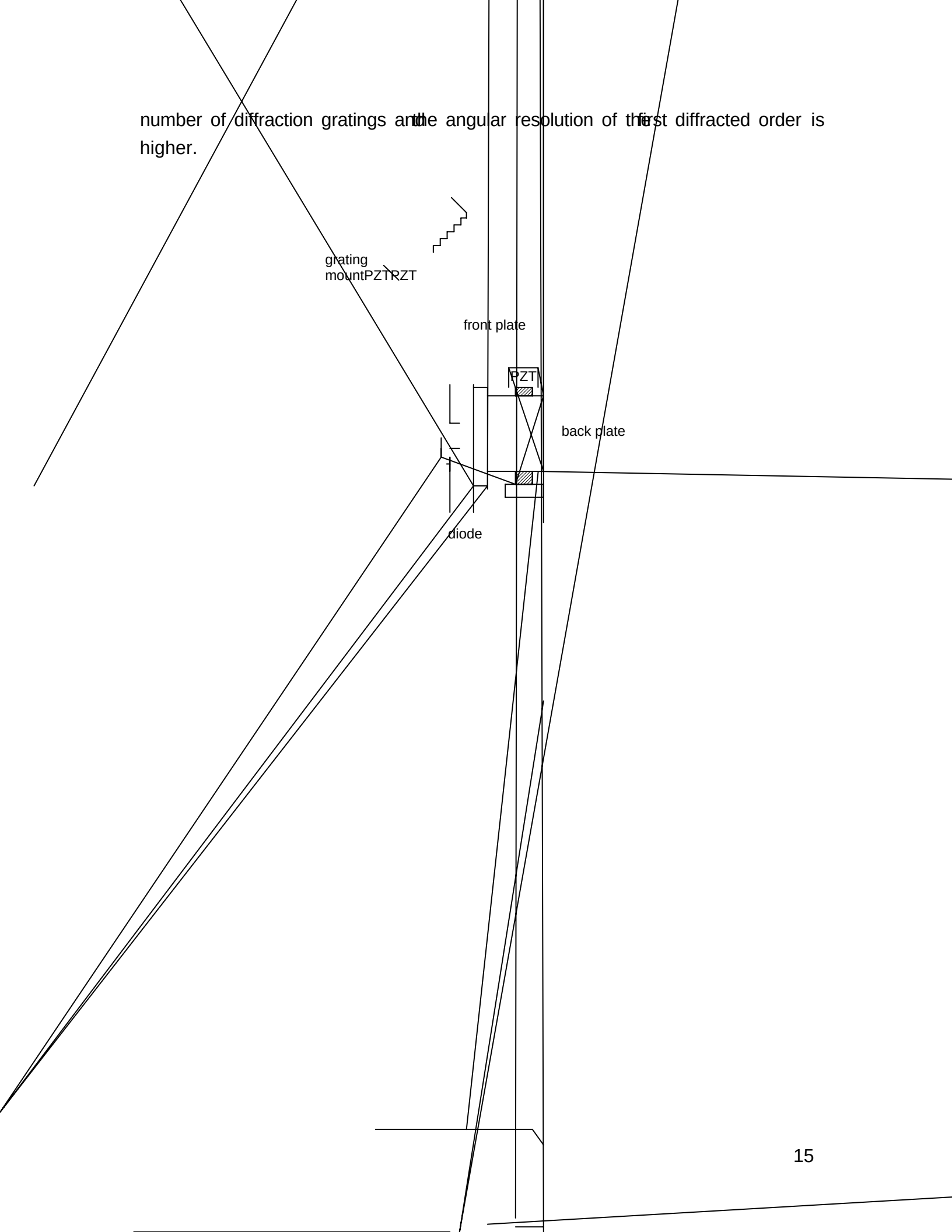

transmitted intensity below the detection limit of a standard photodiode. Once this is done, the isolator body can be turned around in its mount to the forward orientation and rotated to maximize its forward transmission.

Following the isolator, the laser beam passes through a periscope arrangement of mirrors. The periscope serves to increase the beam height to a more manageable level and provides the steering necessary for the following optical elements. Adjusting the bottom mirror allows translation of the beam, while the top mirror allows adjustment of the angle. The 9151 kit from New Focus and two 5102 dielectric near infrared mirrors were used to construct the telescope. It was necessary to make an adapter plate which holds the periscope pedestal on the optical rail. A New Focus 9771 mount holds an uncoated piece of glass in the beam and reflects 8% of the beam into the spectroscopy setup, which is described below.

Following the periscope, the beam is expanded with a two-lens telescope. The first lens is a Newport F-L 20 B diode laser objective with an 8.18 mm focal length mounted in a package with a standard RMS microscope objective thread. Approximately 70 mm away the second lens, a Newport KPX 178 with a 62.9 mm focal length is mounted. The telescope provides a total magnification of 7.7 which produces a beam roughly an inch in diameter. The collimation of the beam is easily adjusted by sending it a long distance (typically several meters) and observing the spot while moving one of the lenses.

The expanded beam is reflected off of two steering mirrors, through a quarter wave plate, and into the pyramidal trap. After passing through the isolator the beam is linearly polarized to a high degree, so it is possible to produce light that is very well circularly polarized with the quarter wave plate. Alignment of this plate is straightforward when the specially-built circularometer is used. This device consists of a spinning polaroid film in front of a photodiode. If light of perfect circular polarization is incident on the detector, the orientation of the polaroid should not affect the intensity seen by the photodiode. If there is some degree of ellipticity present, some orientations of the polaroid will be more transmissive than others and the photodiode will produce a sinusoidal signal. To produce a circularly polarized beam we merely rotate the quarter wave plate until the sinusoid is minimized.

Polarization Spectroscopy

Polarization spectroscopy [Corwin *et al.* 1998] is one of the recent developments in atom trapping that has made this project possible. Our spectroscopy setup consists of a few simple elements using a single laser beam whereas a saturated absorption setup requires several elements and multiple beams. Furthermore, the locking signal from polarization spectroscopy has a much wider capture range than a saturated absorption signal. This makes the system much more robust and therefore better suited to operation outside a laboratory environment.

Theory

At the heart of our spectroscopy set-up lies a room-temperature rubidium vapor cell in a weak (100 Gauss) magnetic field. This magnetic field breaks the spin-degeneracy of the F'= 2, 3, 4 energy levels through the Zeeman effect. Without this Zeeman splitting, left- and right- circularly polarized light will be resonant with an atomic transition at the same frequency. As the magnetic field shifts m_F= -1 down and m_F= +1 up, light that is right-circularly polarized will be resonant at a higher frequency, and left-circularly polarized light will be resonant at a lower frequency. If we subtract the absorption profiles of left- and right-circularly polarized beams, we get a differential signal that crosses zero as the laser frequency is swept across the transition.

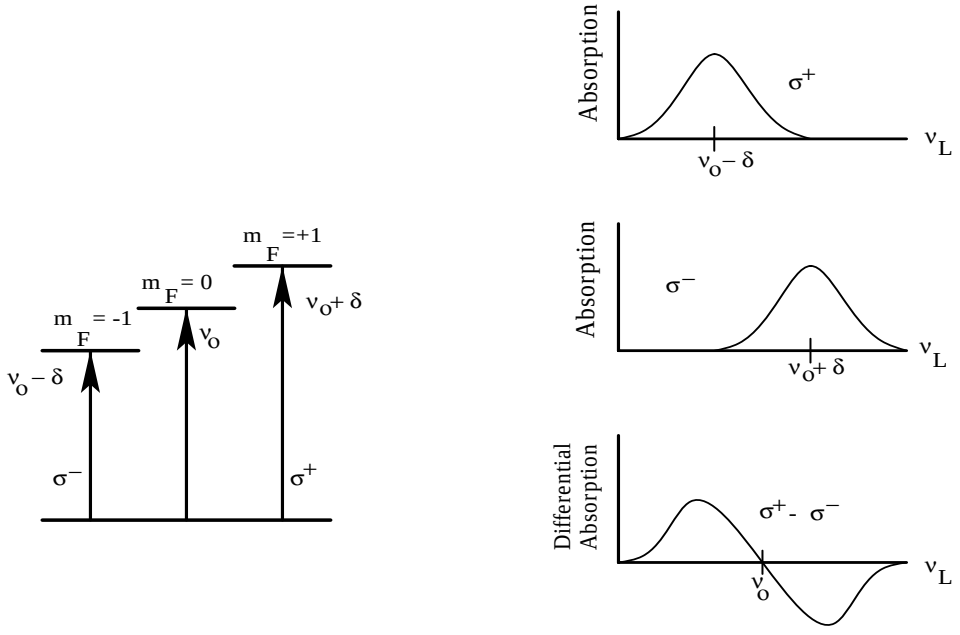

Figure 12 Polarization spectroscopy with the Zeeman shift [Corwin *et al* 1998}

In practice it is not necessary to use multiple beams of light since a single linearly polarized beam can be considered a superposition of two beams with opposite circular polarizations. We may then use a quarter wave plate and a polarizing beam splitter to separate the two circular polarization states and send them to separate detectors. A simple mathematical analysis shows how this is done.

We start with a beam propagating in the z direction with a linear polarization oriented at 45° with respect to the x and y directions.

$$\vec{E} = \frac{\hat{x} + \hat{y}}{\sqrt{2}}$$

Rewrite this in terms of two circular polarization states:

$$\vec{E} = -\hat{r}_+ e^{-i\pi/4} + \hat{r}_- e^{+i\pi/4}$$

where $\hat{r}_\pm \equiv \mp(\hat{x} \pm i\hat{y})/\sqrt{2}$.

After passing through the vapor cell, two new terms have been added: an absorption coefficient α and an index of refraction coefficient ϕ.

$$\vec{E} = -\hat{r}_+ e^{-i\pi/4 + i\phi_+ - \alpha_+/2} + \hat{r}_- e^{+i\pi/4 + i\phi_- - \alpha_-/2}$$

This can be rewritten in terms of the linear polarization states x and y:

$$\vec{E} = \hat{x}\frac{1}{\sqrt{2}}\left(e^{-i\pi/4 + i\phi_+ - \alpha_+/2} + e^{+i\pi/4 + i\phi_- - \alpha_-/2}\right) + \hat{y}\frac{1}{\sqrt{2}}\left(e^{-i\pi/4 + i\phi_+ - \alpha_+/2} - e^{+i\pi/4 + i\phi_- - \alpha_-/2}\right)$$

.

The quarter wave plate and polarizing beam splitter separate these two components and we measure the intensity difference between them with two detectors.

$$I_x - I_y = |E_x|^2 - |E_y|^2 = 2e^{-(\alpha_+ + \alpha_-)/2}\sin(\phi_+ - \phi_-)$$

Since the magnetic field is relatively weak, the Zeeman shift in the energy levels is quite small so ($\alpha_+ + \alpha_-$) and ($\phi_+ - \phi_-$) are also small and we can approximate.

$$I_x - I_y \cong 2\left(1 - \frac{\alpha_+ + \alpha_-}{2}\right)(\phi_+ - \phi_-)$$

We find that the differences in the indices of refraction, as well as the differences in the absorption coefficients, lead to a linear change in the difference signal $I_x - I_y$ near resonance. When on resonance $\alpha_+ = \alpha_-$ and $\phi_+ = \phi_-$ so the difference signal falls to zero, as desired.

Construction and Analysis

An uncoated microscope slide is fixed to a New Focus 9771 Econo-mount and used as a beam pick-off. This light is sent back over the top of the laser and through a half-wave plate (Meadowlark RHM-050-780). Since the output of the anamorphic prism pair is linearly polarized in an unknown direction, the half-wave plate is necessary to impart the correct orientation. The beam passes through a Rubidium vapor cell placed in a magnetic field of 100 ± 10 Gauss. This field is produced by a series of rings carved from a rubber material that has been impregnated with magnetized ceramic. The number of rings and their spacing was adjusted until we achieved the desired field strength and uniformity. Following the vapor cell, the beam passes through a quarter-wave plate (RQM-050-780) and a polarizing beam splitter cube (Melles Griot 003 PBB 011). The two beams that leave the cube then illuminate two Hamamatsu S2387-66R photodiodes. Subtraction of the two photocurrents is done automatically by connecting the two diodes in parallel with opposite polarity.

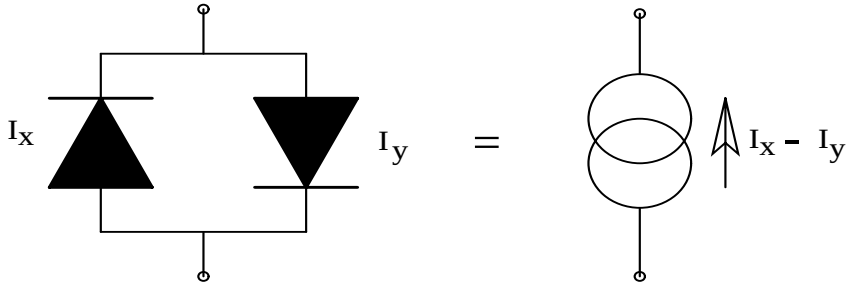

Figure 13 Orientation of photodiodes in polarization spectroscopy set-up

The quarter-wave plate, beam splitter and photodiodes are all mounted on a single Thorlabs C4W cube. The beam splitter sits on a kinematic mounting platform (B4C) in the center of the cube so that the beams can be steered onto the photodiodes. The diodes are glued on blank cover plates that have been modified to hold them, and the quarter-wave plate is held in a lightly modified LM1-A slip ring holder.

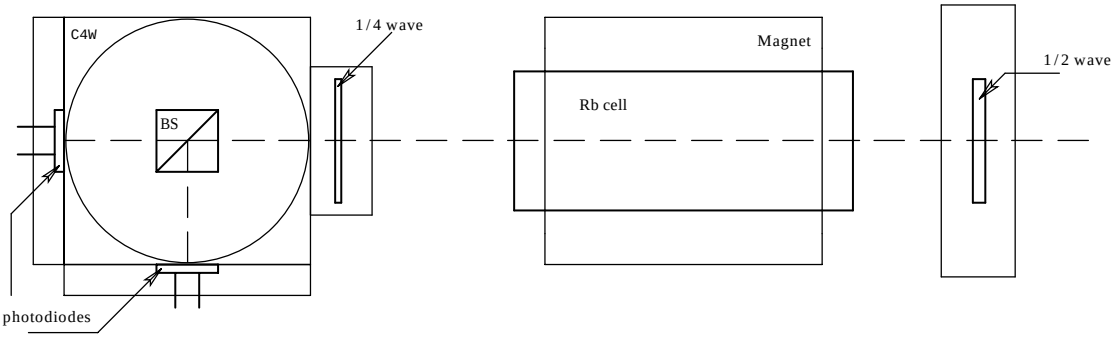

Figure 14 Polarization spectroscopy apparatus, seen from above

Alignment of the spectroscopy optics closely follows the procedure outlined in Corwin et al. When the laser produces a strong fluorescence signal, the quarter-wave plate is removed and the half-wave plate is rotated until a signal appears across the photodiodes. This occurs when the fast axis of the retarder is roughly aligned with the vertical axis of the beam splitter. The quarter-wave plate is then installed and rotated until the spectroscopy signal returns and is centered around zero volts. It is important to recognize that two similar-looking signals can appear at two different orientations of the quarter-wave plate. If the plate is misaligned by exactly 45°, it will create a spectroscopy signal whose peaks line up with the broad absorption features of a saturated absorption signal. This is undesirable, since we wish to create a signal that crosses zero when the saturated absorption signal is peaking. When first aligning the system it is necessary to compare the polarization spectroscopy signal with a saturated absorption signal to ensure that the peaks are indeed out of phase with each other.

The stability of any locking system is limited by the slope of its input signal: if small changes in frequency lead to a large change in the error signal, the locking circuit can easily correct for the frequency change. In a saturated absorption setup the error signal is usually generated by differentiating the sharp peaks in the Doppler-free absorption signal. In the polarization spectroscopy set-up the error signal is the differential absorption spectrum discussed above. Both methods yield roughly the same slope: saturated absorption peaks are small but very sharp, whereas the differential absorption signal is broader but much larger. We have found that the output frequency of our laser is stable to 5-10 MHz, which has proved more than adequate for trapping.

Electronics

A magneto-optical trapping system requires a fair amount of control circuitry, ranging from lowly power supplies to sophisticated feedback loops. Some of these circuits were purchased ready-made; others required design and construction. In the interest of portability, we placed all control electronics in a specially-made box that folds up for storage. Figure 15 provides an overview of the circuits involved.

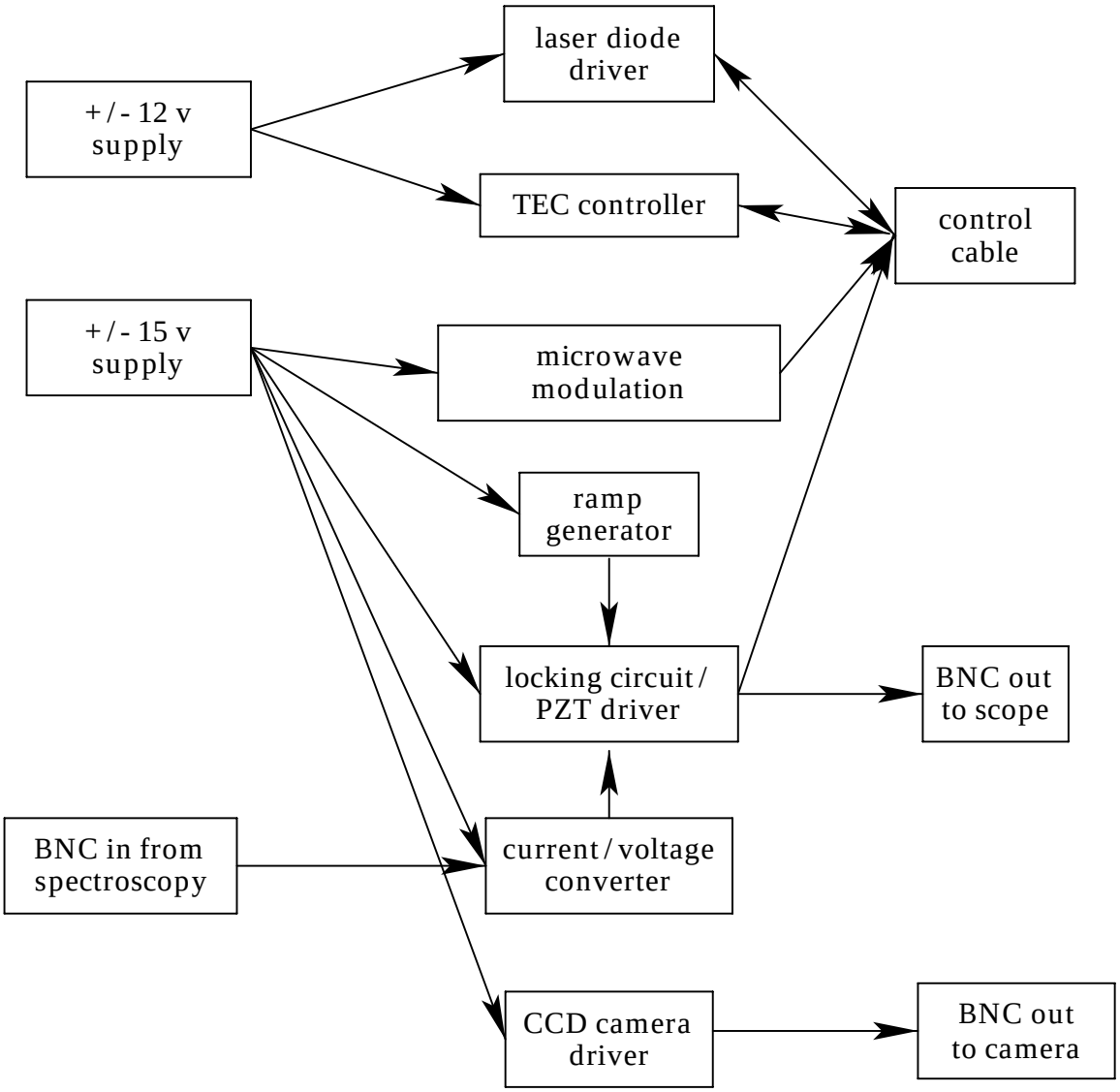

Figure 15 Overview of control electronics

BNC connections are supplied for the spectroscopy input, output signals to an oscilloscope and monitors for many of the circuits. The entire collection is powered from a standard 110 Volt, 60 Hz plug. All connections to the laser head are made through a 15 pin D-subminiature ribbon cable.

1	Laser Anode (gnd)	6	Thermistor	11	+Vtuning for VCO
2	Laser Cathode (-V)	7	Thermistor	12	+15 V for amplifier
3	Photodiode	8	PZT ramp	13	NC
4	TEC +	9	Modulation gnd	14	NC
5	TEC -	10	+15 V for VCO	15	PZT ground

Power supplies

Two bipolar regulated power supplies provide power to all the control electronics. Both employ printed circuits designed and made by the Physics Electronics shop. The +/- 12 volt supply is capable of delivering 700 mA to both its positive and negative terminals, while the 15 volt supply can deliver up to 610 mA. Both sides of both supplies have overload indicator lights that turn on when these current limits are reached.

Laser Diode Driver

Laser diodes of the type used in this experiment must be driven with a constant current power supply. Since the frequency of the laser output depends strongly on the driving current, the supply must be very stable and easily adjustable. We elected to use the Thorlabs LD 1250 laser diode driver. This inexpensive driver supplies currents up to 250 mA and is stable to a few microamps. It comes as a printed circuit board to which various connections must be made.

As is clear from the pin connections, this driver was designed to drive negative-supply diodes. It operates by holding the anode at ground and pulling current from the cathode. This scheme is less than ideal for positive supply diodes, such as our Sharp LT 025 MD models, which have the cathode permanently connected to the diode can. To use this power supply it was necessary to electrically isolate the laser head from the optical rail so that the diode canister could be held at a negative potential. This arrangement leaves the diode somewhat more susceptible to damage from electrostatic discharge. The user must take care not to connect the diode canister to an external ground source, as this is likely to destroy the diode.

Another unfortunate consequence of the driver design is the inability to monitor the current from the photodiode. Indeed, it is important that the photodiode not be connected to the power supply, since any current it produces will be directed through the laser diode.

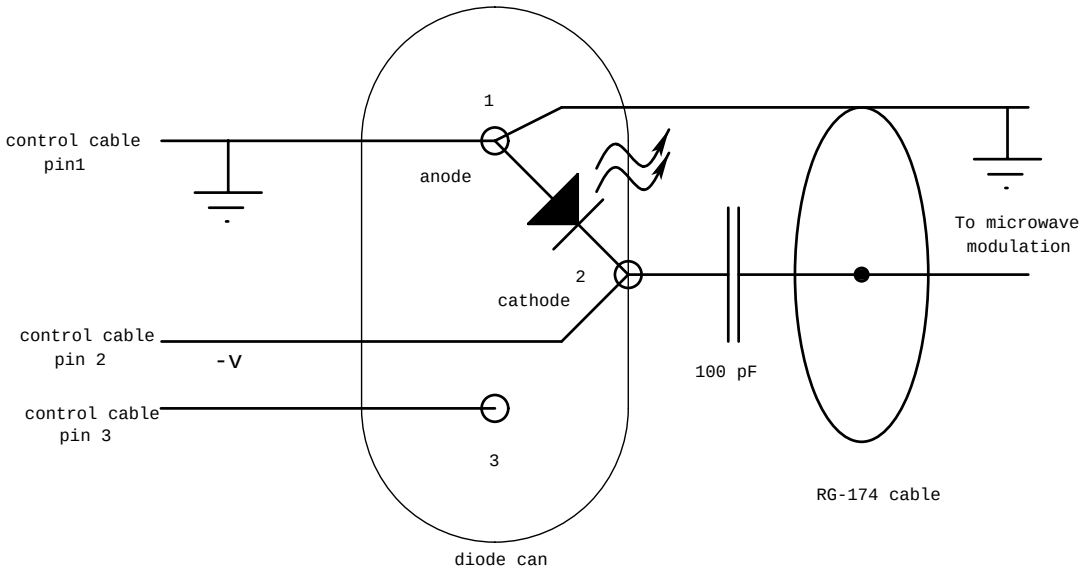

Figure 16 Power connections at laser diode

The output current can be set by the on-board potentiometer and by an external voltage reference applied to pin 4. The total current supplied to the diode is given by

$$I_{LD} = I_{\text{on board pot}} + \left(50 \times V_{\text{pin 4}}\right).$$

A voltage divider circuit applies an adjustable voltage to pin 4 so that the laser current can be fine tuned from the front of the box. Coarse adjustments can be made with the on-board potentiometer accessed through the back of the box. In its present configuration, the on-board pot is set to supply 60 mA of current whenever the supply is on. This can be increased with the helipot on the box up to 140 mA, which is below the damage threshold of the diode.

Thermoelectric Cooler Controller

The output wavelength of the laser diode is also a strong function of its temperature. As discussed above, the laser is cooled by a thermoelectric cooler (TEC) which uses the Peltier effect to pump heat from one of its faces to another. These devices draw a significant amount of current (generally a few hundred milliamps) at relatively low voltage. The current they are supplied determines the amount of heat transferred from one face to the other. We elected to drive the TEC with a Wavelength Electronics PID-1500 temperature controller.

This device contains a feedback loop that seeks to stabilize the signal from some temperature sensor by changing the power supplied to a TEC. We used a Fenwal 121-503JAJ-001 thermistor whose resistance in kilohms is roughly 97 – 2T if T is in °C.

Specifying the desired resistance of the thermistor sets the temperature. This is easily done with the "temp set" potentiometer on the back of the PID-1500 and monitored at the "temp set" BNC connection. The actual resistance of the thermistor can be monitored at the "act temp" connection. Both monitors output a voltage that is equal to the "sensor" dip switch setting times the resistance. The unit works best with the 10 µA switch set, so a voltage reading in millivolts should be divided by ten to get the resistance in kilohms.

Connections to the TEC and the thermistor are made through the control cable. The thermistor has no polarity, but the TEC must be connected in the proper orientation. The red lead is positive, the black one is negative, and both are soldered to the side that gets hot. After installation, the stability of the controller was tested by monitoring fluctuations in the thermistor's resistance. This resistance was seen to stray by about 20 , which corresponds to temperature changes of a few millikelvin, which is suitably stable for trapping.

CCD Camera

To display the trap on a television screen we use a Watec WAT-660D CCD camera. This device requires a stable voltage between 9 and 9.9 Volts and outputs a standard video signal. Since we only have 12 and 15 volt supplies available, it was necessary to construct a voltage regulator. With Mike Murray's help, the following circuit was designed and built.

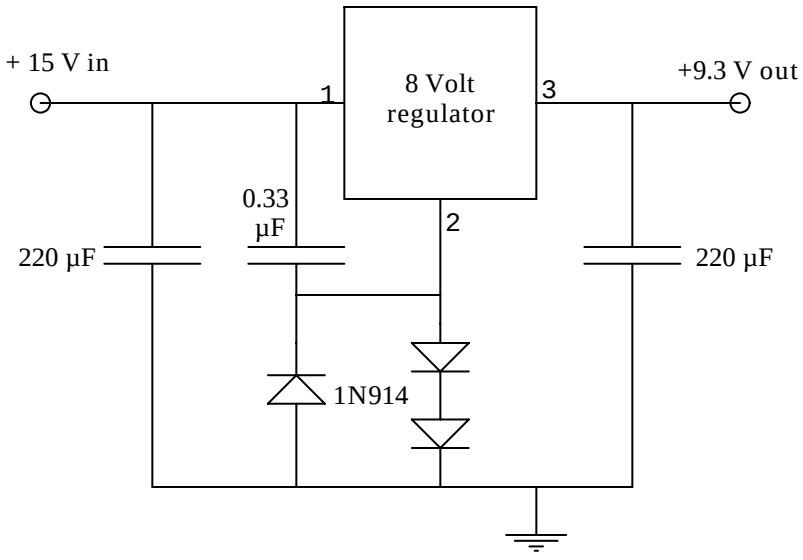

Figure 17 CCD camera power supply

The two series 1N914 diodes hold the "ground" pin of an eight-volt voltage regulator about 1.3 volts above ground, so that its output is about 9.3 volts. The other diode and the capacitors serve to filter out turn-on spikes and noise. This circuit is contained in small enclosure mounted near the camera, and powered by a BNC cable supplying +15 V from the main electronics box.

Microwave Modulation

This apparatus uses a microwave modulation setup similar to that described by Feng and Walker [1995]. Atoms are pumped from the $5^2S_{1/2}$ F=2 state to the $5^2P_{3/2}$ F=3 state by inducing sidebands on the laser output spectrum which are resonant with this transition. This is done by producing a modulating signal at 2.9 GHz with a voltage-controlled oscillator (VCO), amplifying this signal, attenuating it a bit, and then applying it to the laser diode.

We use a model VTO-8240 oscillator in a TF-801 test fixture from Avantek to produce the signal. Earlier work with this unit determined that it produces the appropriate frequency when the tuning voltage is 8.54 volts. This voltage is set inside the electronics box with a standard voltage divider circuit containing a potentiometer and a resistor. A BNC receptacle allows monitoring of the tuning voltage. It is worth noting that this voltage-divider arrangement makes the output voltage rather sensitive to the exact value of the power supply. If a different 15 volt power supply were to be used, it would be necessary to adjust the potentiometer to compensate for any deviation from 15 volts.

The microwave signal is amplified by approximately 8.3 dB with a Cougar AC3579C amplifier. This produces a signal that is strong enough to induce mode-hops and other unpleasant behavior from the laser diode, so attenuation is necessary. We have found that it is possible to stabilize the laser with as little as 5 dB of attenuation, but it is possible to get a trap with as much as 20 dB. Since we would like to minimize the amount of power put in the sidebands while still trapping, we use the 20 dB attenuator.

Both the VCO and the amplifier are powered by + 15 volts and ground. It is important to note that the amplifier must be turned on first and off last-- it is always better to amplify nothing than to drive a dead amplifier. The two power connections have been made so that it is not possible to have the VCO on while the amplifier is off.

Following attenuation the microwave signal is fed into the laser diode. Because we are in the unusual situation of having the anode at ground and the cathode negative, it is necessary to connect the microwave signal backwards-- the signal is applied to the cathode, not the anode as in Feng and Walker. This implies that we are not only driving the diode, but the entire canister as well (see Figure 16). It is difficult to say how this affects the coupling efficiency into the diode-- all we know for certain is that it works.

Ramp Generator and Current to Voltage Converter

The wavelength of the laser output is determined by the angle of the diffraction grating, which in turn is determined by the voltage applied to the piezoelectric translator. It is often helpful to repeatedly scan the laser frequency across resonances, for which we need to drive the PZT with a sawtooth-shaped signal. For this we used the ramp generator designed by Steve Kadlecek. At its heart is an ICL 8038 oscillator that creates a periodic ramping signal, the frequency of which is easily controlled with an external potentiometer. This signal is then amplified by an op-amp whose gain is adjustable with another potentiometer. A third potentiometer and two more op-amps allow a variable dc offset, and a unity-gain buffer can be inserted to invert the output. The ramp signal is sent to a monitor BNC on the front of the box, a scope triggering output on the top, and to the locking circuit.

The amplitude and dc offset of the ramp sent to the PZT can be changed at the ramp generator and at the locking circuit. We have found that it is most convenient to set the output of the generator symmetric around zero (no dc offset) and approximately ± 5 volts in amplitude. The frequency should be chosen so that one full sweep fills up a 10 ms scope trace. Once these are set, it is best to change the dc offset and gain at the locking circuit and leave the ramp generator alone. This makes it easier to understand the operation of the locking circuit and reduces the likelihood of saturating one of the amplifiers.

We used the standard current to voltage converter designed by Krista Mullman and transferred to printed circuit board by Art Webb. It places the current from the spectroscopy setup into the feedback loop of an op-amp. As the op-amp seeks to equalize the voltages at its inputs, its output voltage follows the input current. By adjusting the resistance in that feedback loop, one is able to adjust the gain of the converter. A five-position switch allows five different resistors ranging from 1 k to 5 M to be inserted into the loop to achieve the desirable gain. A potentiometer and another op-amp change the

bias on the converter, allowing adjustment of the dc offset of the output signal. This output is fed into the locking circuit and can be monitored at a BNC receptacle on the box.

Locking Circuit

Frequency stabilization of the laser is accomplished by the locking circuit. It reads the spectroscopic signal from the current to voltage converter and generates an error signal corresponding to fluctuations in the laser frequency. When set to "lock" the circuit uses a feedback loop to minimize the error signal by changing the voltage applied to the piezoelectric transducer. When set to "ramp" it drives the PZT with the sawtooth wave made by the ramp generator.

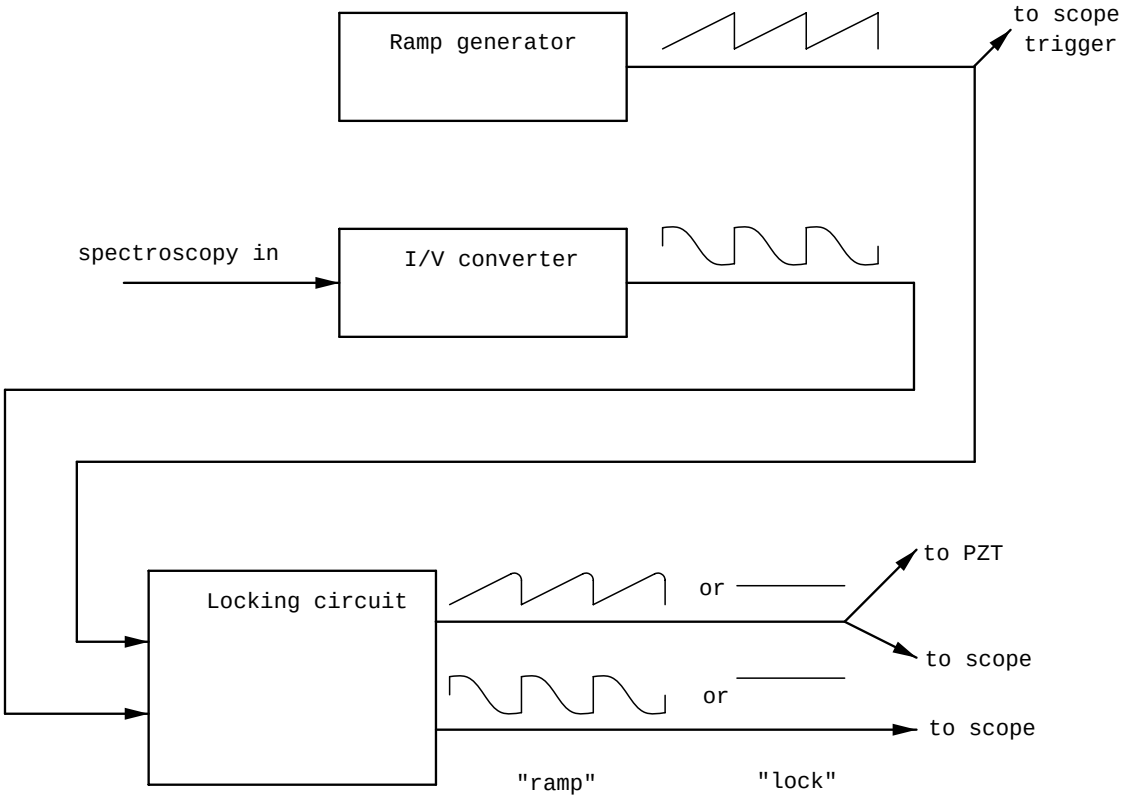

Figure 18 Locking circuit schematic

We use the locking circuit designed by Rob Williamson, even though it was intended to use a saturated absorption signal as the spectroscopic input. Using our polarization sensitive spectroscopy setup substantially simplifies the operation of the locking circuit. The output from a saturated absorption setup consists of sharp peaks corresponding to a Doppler-free absorption profile. Since the locking circuit is only able to lock to a zero-crossing signal, a lock-in amplifier is necessary to differentiate the sharp peaks and generate zero-crossings. In contrast, the polarization sensitive spectrometer

automatically produces a signal that crosses zero and eliminates the need for a lock-in amplifier.

In both the ramp and lock modes, the circuit allows the user to adjust the horizontal and vertical offset of the PZT driver and the gain of the feedback loop. The horizontal offset scrolls the spectrum left and right so that the desired features lie in the center of the ramp. The vertical offset sets the relative position of the zero crossing, and thereby controls the frequency of the lock. In the ramp mode, increasing the feedback gain increases the range of frequencies over which the laser will sweep. When locking, a higher gain increases the stability of the lock, up until the point at which the feedback loop begins to oscillate. Since there is only one zero crossing in the polarization spectroscopy signal, as opposed to one for each absorption peak in the SA signal, it is not necessary to turn the gain way down before switching from ramp to lock.

The last stage of the locking circuit is an integrator with a relatively long time constant. This serves to filter out any high frequencies in the signal to the PZT and prevent undue stress. In particular, the integrator rounds off the edges of the sawtooth wave and reduces ringing of the spring in the laser head.

Vacuum System

Design

A vacuum system suitable for use in magneto-optical trapping must meet several criteria. It must contain a supply of rubidium, preferably behind a valve. It must have a mounting surface for the funnel assembly and a window for the trapping laser. And it must be able to achieve and maintain pressures around 10^{-8} torr. Meeting these criteria while minimizing the size and weight of the vacuum system proved to be a challenge.

Pumping a chamber down from atmospheric pressure to 10^{-8} torr typically requires a turbomolecular pump backed by a roughing pump. These pumps cost thousands of dollars and weigh well over twenty pounds, so we elected to install a smaller holding pump on the chamber and use a valve for temporary connection to a turbopump. With this arrangement the chamber can be attached to a powerful pumping system and evacuated to the desired pressure, then the valve can be closed and the chamber removed.

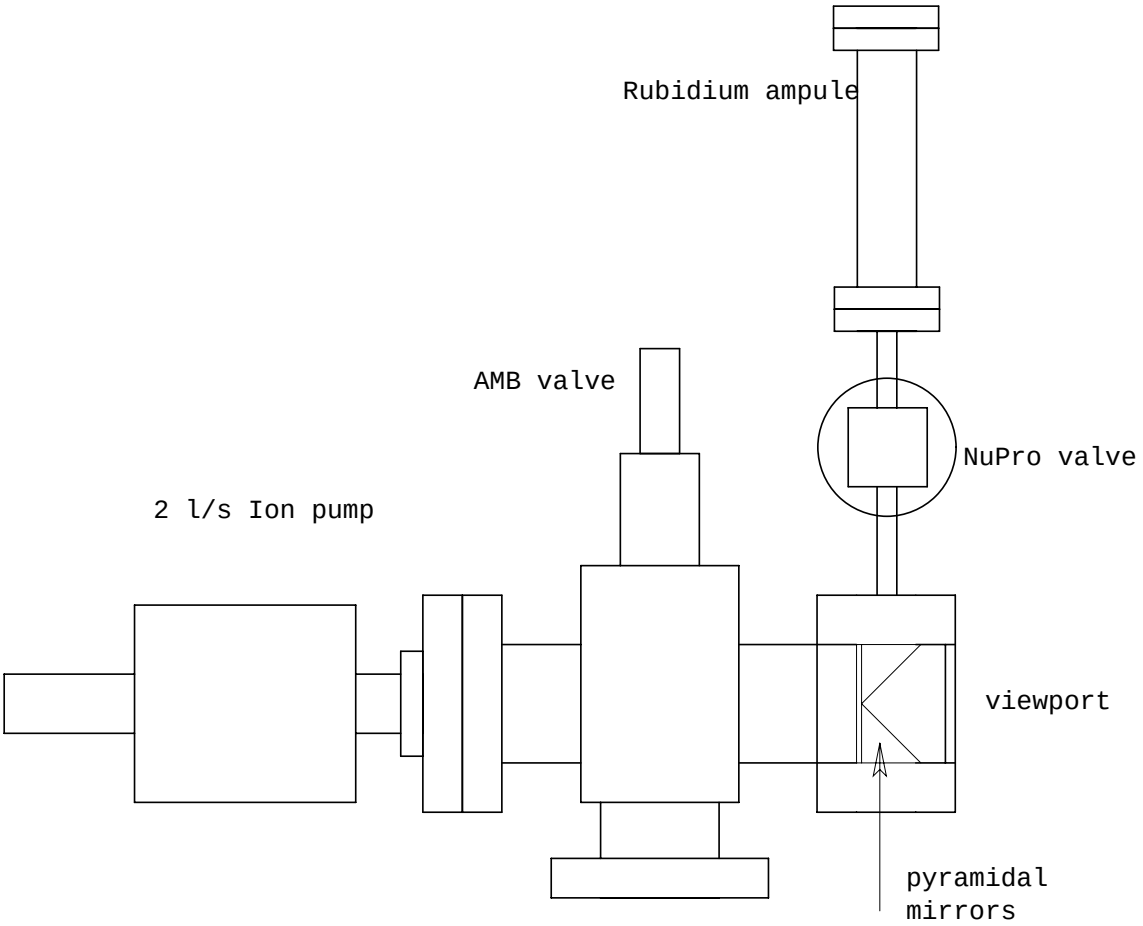

Figure 19 Vacuum chamber, seen from above

We chose a 2 liter per second Ion pump from Duniway with a 1.5 inch conflat-style flange. Duniway sells this pump under the name VA2-MINI-VAC-B, and it is comparable to the 913-5000 pump sold by Varian. To reduce weight and prevent stray fields from disturbing the trap, we used the high-quality Samarium Cobalt magnets (Duniway MAG-0112 or Varian 911-0030) instead of the more common Alnico variety. This pump is powered by a Varian MiniVac Controller, which produces up to 5 kV and can be operated at any pressure.

The all-metal bakeable (AMB) valve (Varian 9515017) has two 2.75" ports that are always connected and a third that can be closed off. We use the two ports to permanently connect the ion pump with the pyramidal mirrors and the third for temporary connection to a turbopump. The pyramid assembly is mounted to a blank conflat gasket that has several large holes to allow adequate conductance of Rubidium from the trapping area to the pump.

The pyramid sits in a double-sided conflat flange onto which a glass viewport is mounted. A small vial of Rubidium is stored in a three inch conflat nipple that is connected by means of a valve (NuPro SS-4H-TH3) to the double-sided flange.

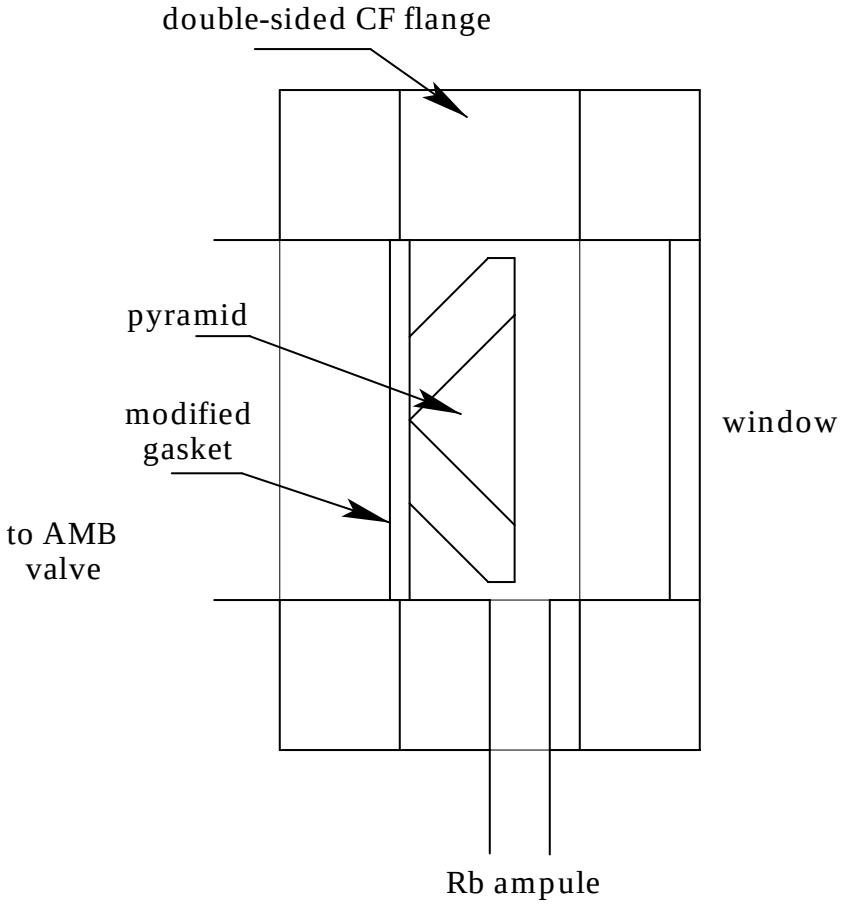

Figure 20 Close-up of funnel assembly in vacuum chamber

Gas Load Analysis

To maintain an ultra-high vacuum, the conductances between adjacent areas of the chamber must be at least as high as the pumping speed. Otherwise we cannot assume that the pressure is in equilibrium throughout, and the pump performance will be severely reduced. Since the maximum pumping speed is only 2 L/s, this is not a difficult criterion to meet. Indeed, the only region where this is a concern is at the rim of the pyramidal mirror assembly. The atoms must flow through a gap between the wall of the chamber and the edge of the pyramid that measures less than two millimeters. To see if the conductance through this gap is adequate, the following calculation is necessary.

In Vacuum Technology (Roth, 1982, p. 88) an equation is given for the conductance of a short tube of annular cross section. If D_o and D_i are the inner and outer radii, and L is the length,

$$C = \frac{12.1(D_0 - D_i)^2(D_0 + D_i)K_0}{L + 1.33(D_0 - D_i)}$$

where C is the conductance for air at 20°C. Ko is a correction factor determined by the ratio D_o/D_i. In our case, D_o = 3.81 cm, D_i = 3.429 cm, L = 0.279 cm and K_o = 1.43. These numbers yield a conductance of 23 L/s, which ensures equilibrium in the chamber.

Construction and Characterization

Prior to assembly all the vacuum components excepting the AMB valve were thoroughly cleaned. We employed the standard cleaning routine for stainless steel in ultra-high vacuum-- a succession of baths in Oakite, ethanol, acetone and distilled water. We then assembled the components, taking care to prevent fingerprints or other grease from getting inside. We connected the chamber to an Alcatel Drytel MicroHV turbopump and a calibrated ion gauge. We pumped down to 2.4 x 10^{-7} torr at room temperature and then began to bake out. Following Renée Nesnidal's advice, we covered the glass viewport with several layers of aluminum foil to reduce thermal stress and applied a thermocouple (51.4 μV/°C) to the chamber to monitor its temperature. The chamber was baked at about 175°C above room temperature for seven days. During that time the pressure rose to 3.2 x10^{-6} torr and then fell to 1.6 x10^{-8} torr.

These pressure measurements were made by the ion gauge with the turbopump operating, and were therefore subject to large systematic errors. It is also possible to measure the pressure in the chamber by monitoring the current on the ion pump; if more atoms are present in the chamber the pump will draw more current. The MiniVac pump controller provides a current monitor but it is not designed for operation at such low pressures and is not well calibrated. Indeed, the monitor is often at a negative voltage, which would imply a negative pressure if we believed the stated calibration. After a few failed attempts to trap rubidium, we decided to calibrate the ion pump's current monitor and thereby get a better sense of the pressure in the chamber.

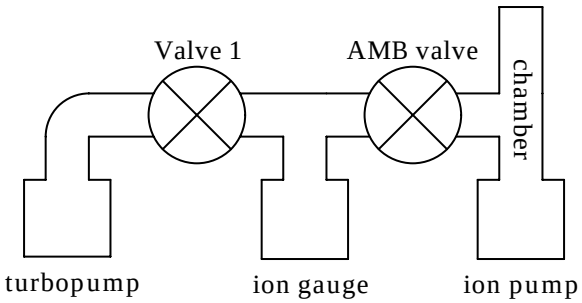

Figure 21 Ion pump calibration schematic

We connected the chamber to Ian Nelson's vacuum system, which has a valve (V1) between its turbopump and ion gauge. With the AMB valve closed and V1 open, we first pumped the ion gauge down to about 3 x 10^{-6} torr. We then closed V1 and opened the AMB valve, so that the ion gauge and ion pump were at the same pressure. We then recorded the pressure read by the ion gauge and the current drawn by the ion pump as the pressure fell. The resulting data suggest that the pressure is approximately given by

$$P = [(0.534 \times \text{Voltage}) + 0.33] \times 10^{-7} \text{ torr}$$

when the monitor voltage is measured in millivolts.

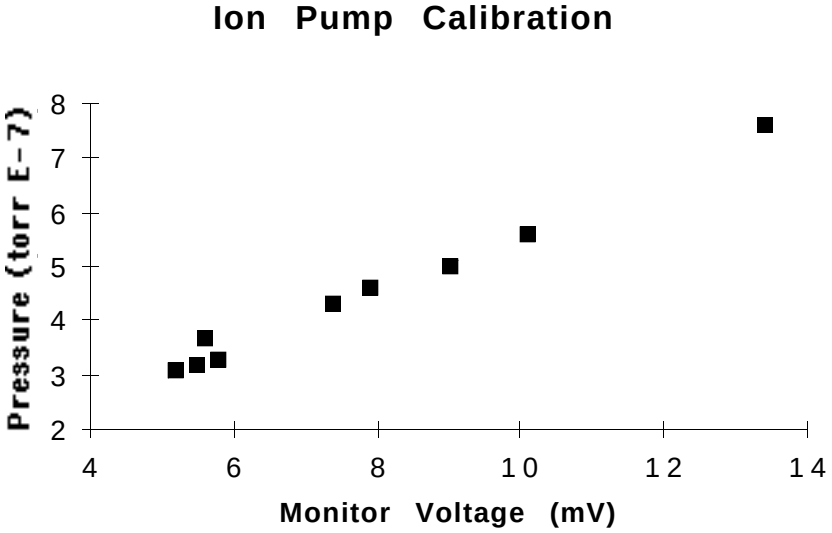

Figure 22 Ion Pump calibration

Since we typically run with a nominal monitor voltage of 0.0 to -0.9 mV we believe that the pressure in the chamber is below 3 x 10^{-8} torr, which is quite suitable for trapping.

Pyramidal Mirror

The pyramidal mirror assembly forms the heart of our magneto-optical trapping system. It consists of four identical sections bolted together to form a right-angle hollow pyramid. The pieces were designed by Steve Kadlecek and machined from oxygen-free hard copper by the Physics Department Instrument Shop. The reflective surfaces were then highly polished using standard mirror-polishing techniques. To prevent the reflective gold coating from diffusing into the copper, a layer of rhodium was evaporated onto the polished surfaces. A layer of gold was then electroplated onto the pieces by Rocky Mountain Instruments, Inc., and the pieces were evaporatively coated with a layer of silicon dioxide by Beste Sci-Glass. This final layer of SiO_2 helps prevent scratches on the gold surface and shields it from the corrosive effects of rubidium.

The four pieces were then assembled with vented socket screws and mounted to a modified blank conflat gasket. The gasket has four small holes near its center for affixing the pyramid, and eight larger ones (1/4" dia.) around the outside to allow conductance from one side of the pyramid to the other. The assembled pyramid and mounting gasket were then placed in a bakeout chamber, pumped down to a few millitor and held at 200° C for two hours.

When assembling the pyramid we took care to get the interior angles as close to 90° as possible. After placing the funnel under vacuum and failing to get a trap, we began to suspect that mirrors were misaligned. By measuring the angle between a laser beam and its reflection from two mirrors, we measured the angles between all the mirrors. We found that the left and right mirrors are separated by 90.3°, and the top and bottom mirrors are separated by 91.0°. This makes our pyramid comparable to the larger pyramidal funnel that has been successfully used to make a MOT for potassium. We also measured the reflectivity of our pyramid by measuring incident and reflected laser intensity. We found it to be around 93% for two reflections, again comparable to the potassium funnel. Finally, we measured the degree of circular polarization of the reflected light. Reflections off a gold surface at 45° will in theory reverse the circular polarization almost perfectly. In practice, however, birefringence in the chamber window and the SiO_2 coating, and imperfections in the mirror surface will impart a substantial elliptical component to the reflected light. Since the operation of our MOT relies upon appropriately circular light, we were concerned that these imperfections might prevent trapping. Using our circularometer we found that light entering our pyramid was 2% linear, and after two reflections light exiting the pyramid was 20% linear. This compares favorably with the potassium funnel, which returned 60%

linear light. Based on these measurements we concluded that our pyramid is suitable for successful trapping.

Permanent Magnets

Our first demonstration of a magneto-optical trap with this apparatus employed two current coils in the anti-Helmholtz configuration. These coils, built by Renée Nesnidal and Steve Kadlecek, are about 10 cm in diameter and have approximately 50 turns of wire each. Using a gaussmeter we found that the desired field gradient of 10 G/cm is created at the center when 4 A is supplied to the coils. These coils work very well and we were able to establish a stable trap with them. However, a power source capable of providing 4 amps is likely to be cumbersome, so we sought a way to create the same magnetic field with permanent magnets. Bien Chann suggested a simple configuration of permanent magnets which has proved very successful. By rolling a length of flexible magnet into a cylinder, so that the interior surface is North and the exterior surface is South (or vice versa), we reproduce the anti-Helmholtz field.

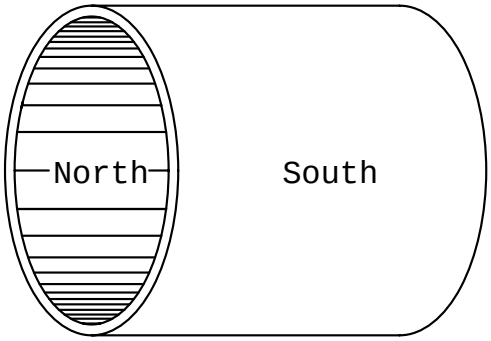

Figure 23 Permanent magnet used to reproduce an anti-Helmholtz field

It is not hard to see how this works if we imagine the magnet as an assembly of tiny current loops all conducting in the same direction. Wherever one loop is tangent to another the currents are travelling in opposite directions, so they cancel. All the loops along the edge of the magnet have no neighbors to cancel with, so they create an effective current around the edge of the cylinder. These effective currents are on opposite ends of the

cylinder so they are in opposite directions and we have reproduced our two coils.

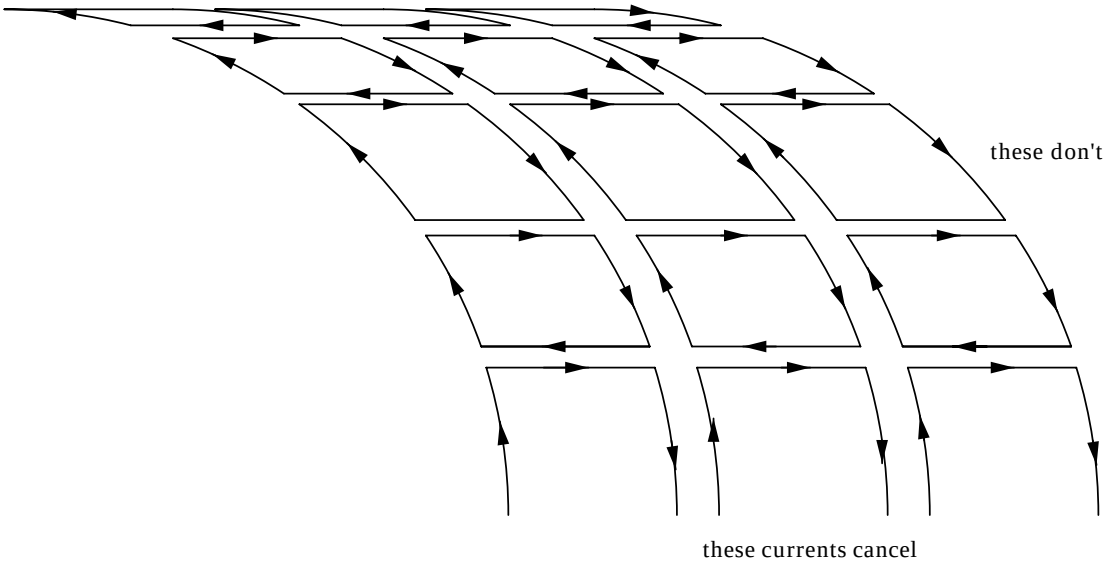

Figure 24 Stokes' construction for field of permanent magnets

We formed this magnet by wrapping a length of rubberized magnetic material around a 5" diameter aluminum cylinder. The appropriate field strength was obtained by milling the magnetic strap thinner until the gaussmeter indicated a gradient of about 12 G/cm. Since the light forces are likely to be unbalanced in the exact center of the pyramid, we use a small magnet to push the location of zero field away from the center.

Set-Up and Use

Once the system has been unpacked and all the necessary electrical connections have been made, we are ready to start turning the system on. Since it takes about 15 minutes to achieve temperature stability, it is best to turn on the TEC controller as soon as possible. It should not be necessary to change the temperature setpoint from its nominal value of 54.8 k on the thermistor, or 0.548 mV on the temp set monitor. After 5 minutes or so, we can turn on the ramp generator and the laser diode driver. One should make certain that the current control on the laser driver is turned all the way down before turning it on. A few seconds will elapse before the supply starts delivering current to the laser, though with the supply turned down it is likely to be below threshold. As the current is gradually turned up past 60 or 70 mA (0.6 to 0.7 V on the monitor) the laser should turn on. With the current turned up to its nominal value of 110 mA, we are ready to search for fluorescence. By placing a rubidium cell in the expanded laser beam and observing it with an IR viewer, we can make small changes in the driving current until fluorescence is seen. Dim flashing in the cell means the laser frequency is close to 780 nm, and we might be able to fine-tune the frequency by controlling the horizontal offset to the PZT. When the laser is sweeping across the correct frequency a very strong fluorescence signal is visible. Since the laser produces approximately 25 mW of power, this flashing is unmistakable—if there is any doubt, the laser is not at the right frequency. If no amount of fiddling with the current control can produce fluorescence, it is necessary to make coarse adjustments to the laser frequency by turning the mirror mount steering screws with an allen wrench. This is extremely delicate work and should be done with care. If the laser frequency drifts away from fluorescence, it likely that the temperature has not yet stabilized and more waiting is in order.

It is currently necessary to add rubidium to the vacuum chamber whenever trapping. This is done by heating the NuPro valve with a heat gun for a few minutes until fluorescence is seen in the chamber. It is important to stop heating the chamber once flashing is visible with the CCD camera. When loaded, the chamber is likely to retain a trappable level of rubidium for several hours.

Once florescence has been achieved, a differential absorption signal should be visible from the spectroscopy setup. It is helpful to turn the gain of the locking circuit down fairly low so that the laser does not make several mode-hops in a sweep. By changing the horizontal offset of the PZT driving signal we can scan across the two spectral

features produced by absorption from ^{87}Rb and ^{85}Rb. It is often necessary to make small changes in the driving current when scanning like this. In general, a noisy mode-hop that creeps in from one side of the signal means the current is too low; a sudden loss of all spectral features means the current is too high. With a good spectrum on display, we are ready to add microwave modulation. It is very important to turn on the amplifier first, then the VCO—otherwise we risk irreparable damage to one or both components. When the VCO is turned on the power input to the laser crystal changes a little so its temperature is also likely to change. This may induce a mode-hop. If so, it is best to wait a few minutes for the temperature to stabilize, then adjust the current supply to get the spectrum back.

By changing the horizontal and vertical offsets, we can make the spectroscopy signal cross zero on the side of the larger spectral feature.

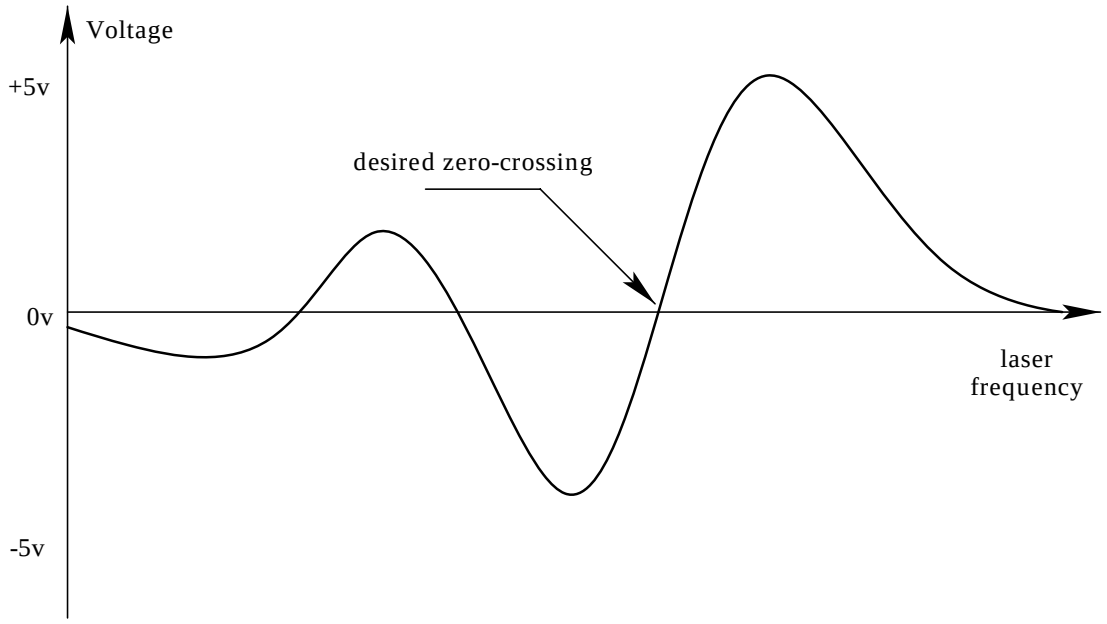

Figure 25 Differential absorption signal [From Corwin *et al*, 1998]

We next adjust the gain of the locking circuit until this is the only zero-crossing on the display and then switch from ramp to lock. The signal should quickly stabilize at zero. By adjusting the vertical offset of the locking circuit we can now change the location of the lock and scan across frequencies until a trap is observed. It may be helpful to wave a small permanent magnet around the chamber so any trap that forms will move around and be more visible.

Conclusions and Outlook

In this project we have created a magneto-optical trapping system for rubidium. Throughout the design and construction of this system we have worked to make it as small and self-contained as possible so that the apparatus may be transported and used outside of a laboratory environment. Additionally, the detachable self-contained laser could be quickly and easily integrated into larger experimental systems.

To this end, we have incorporated several novel techniques that have recently been developed. Chief among these is polarization sensitive spectroscopy, which produces a surprisingly robust frequency-stabilization scheme with relatively few optical components. Pioneered at JILA, this system uses the Zeeman effect to shift the absorption peaks of two circularly polarized beams passing though a rubidium cell and generates an error signal from the difference between the two peaks.

The three orthogonal pairs of counter-propagating laser beams needed for trapping are produced with a right hollow pyramid arrangement of mirrors. This pyramidal trapping scheme significantly reduces the complexity of our optical system and is central to its portability

We have also developed and implemented a simple and effective way to produce a quadrupole magnetic field of the appropriate strength and orientation with a single permanent magnet. This method allows us to eliminate the bulky power supplies necessary when using anti-Helmholtz current coils.

With these techniques and others, we have reduced the weight of the system below 50 pounds and its size within most airlines' checked baggage limits. When properly prepared, the system requires roughly one hour to set up and operate, making it suitable for travelling demonstrations. Although trapping has been achieved on several occasions, some work remains to be done. The 1/4" CCD camera saturates fairly easily, so that the trap appears no brighter than light scattered from dust on the window and mirrors. We believe that an appropriate neutral density filter would improve the visibility of the trapped atoms. Further work on the focusing of the camera is also likely to help. Finally, a custom-fit shipping crate has yet to be made. When these few improvements are made, the system will be ready for testing in the field. This system promises to be a useful and valuable demonstration of modern physics concepts in classrooms, lecture halls and laboratories.

Bibliography

A.S. Arnold, J.S. Wilson, and M.G. Boshier. A simple extended-cavity laser. *Review of Scientific Instruments*. Vol. 69, No. 3, 1236-9, 1998

S. Chu, j. E. Bjorkholm, A. Ashkin, and A. Cable. Experimental Observation of optically trapped atoms. *Physical Review Letters*, Vol. 57, No. 3, pp. 314-7. 1986.

S. Chu and C. Wieman (Eds.), Special Issue, *Journal of the Optical Society of America B*, Vol. 6, pp. 2020- 2270. 1989

K. L. Corwin, Zheng-Tian Lu, Carter F. Hand, Ryan J. Epstein, Carl E. Wieman. Frequency-stabilized diode laser with the Zeeman shift in an atomic vapor. *Applied Optics* Vol. 37, No. 15, 3295-8, 1998

C. J. Foot, Laser cooling and trapping of atoms, *Contemporary Physics*, Vol. 32, No. 6, pp. 369-381. 1991

P. Feng and T. Walker, Inexpensive diode laser microwave modulation for atom trapping, *American Journal of Physics*, Vol. 63, No. 10, 905-8, 1995.

K. I. Lee, J. A. Kim, H. R. Noh and W. Jhe, Single-beam atom trap in a pyramidal and conical hollow mirror. *Optics Letters* Vol. 21, pp. 1177-9, 1996

A. Roth, *Vacuum Technology*. Elsevier Science Publishers, The Netherlands, 1982

C. Wieman and L. Hollberg, *Review of Scientific Instruments*. Vol. 62, No. 1, 1991

R. S. Williamson, Magneto-optical trapping of potassium isotopes, Doctoral dissertation, University of Wisconsin-Madison, 1997

R. S. Williamson III, P. A. Voytas, R. T. Newell, and T. Walker, A magneto-optical trap loaded from a pyramidal funnel. *Optics Express* 1998